ELSEVIER

Ocean Modelling 2 (2000) 29–43

Ocean Modelling

www.elsevier.com/locate/omodol

A priori estimates of mixing and circulation in the hard-to-reach water body of Lake Vostok

Alfred Wüest [a,*], Eddy Carmack [b]

[a] *Applied Aquatic Ecology (APEC), Limnological Research Center – EAWAG, Seestrasse, Kastanienbaum CH-6047, Switzerland*

[b] *Institute of Ocean Sciences, 9860 West Saanich Road, Sidney, BC, Canada V8L 4B2*

Abstract

Lake Vostok in Eastern Antarctica is covered by a ~4000 m thick ice sheet that glides over the subglacial water body on a time scale of ~20 000 years. As a basis for "pre-expedition" planning, a priori estimates are made for water temperature, heat flux and currents. Whereas vertical temperature gradients are predicted to be extremely small due to geothermally driven convective turbulence, horizontal temperature gradients are expected to be present due to the horizontal gradient of the pressure-dependent freezing point at the base of the sloped ice ceiling. Except at the lake's deepest location, where a thin stratified layer may develop, the vertical in situ temperature profile will be near the adiabatic lapse rate. Based on internal heat fluxes associated with observed melting and re-freezing at the base of the ice sheet we calculate internal currents by assuming geostrophic balance. Vertical and horizontal motions are both expected to lie in the range of fractions of mm/s. Ice plasticity (hydrostatic adjustment) and water–ice heat exchanges are predicted to flatten the ice-cover quickly to a remarkably smooth terrain while the ice moves over the lake. These results corroborate well with the recent finding that only the upper part of accreted lake water, retrieved from the Vostok ice-core, contains particles. Our predictions are discussed with respect to uncertainties and the experimental challenges to be met.

1. Introduction

Of all lakes on Earth, Vostok reigns most mysterious. Located in Eastern Antarctica (near 77°S; 105°E) this 10–20 million year-old freshwater body is covered by a 3.7–4.2 km thick layer of glacial ice. Lake Vostok is large: it has an area (~14 000 km^2) near to that of Lake Ladoga, a volume (~1800 km^3) near to that of Lake Ontario, and a maximum depth (~510 m) near to that

* Corresponding author.

E-mail addresses: wuest@eawag.ch (A. Wüest), carmacke@dfo-mpo.gc.ca (E. Carmack).

1463-5003/00/$ - see front matter
PII: S1463-5003(00)00007-X

of Lake Tahoe. Lake Vostok was discovered using remote survey methods (e.g., by airborne radio echo sounding, satellite altimetry, and seismic measurements; see Kapitsa et al., 1996) but no in situ measurements have yet been made (NSF, 1999). There is evidence, however, that the lake is composed of fresh water (i.e., low salinity), that up to 500 m thick sediments cover the lake floor, and that microorganisms that have been isolated from their surroundings for millions of years will be found in their waters and sediments (Karl et al., 1999; Priscu et al., 1999).

The combination of extraordinarily thick ice-cover and extreme isolation of its microorganisms makes Vostok an attractive analog for planetary exploration, as noted in the NASA Europa-Vostok Initiative (F. Carsey, personal communication). Such a work would only be attempted if it could be done without contaminating samples and the water in the lake. This constraint calls for the use of in situ micro-robotic instrumentation specially designed to address an anticipated range of physical and geochemical conditions within Vostok. Our aim here is to outline the physical conditions that future researchers may face while exploring the lake by asking the following three questions:

- Do we expect horizontal and vertical gradients of water properties, and, in particular, how will the density-defining temperature distribution look?
- Do we expect measurable motions within the lake, and how are such potential currents related to boundary conditions?
- What sort of in situ measurement constraints might challenge our ability to detect flow and spatial structure within the Vostok's cavity should penetration be achieved in years ahead?

2. Thermodynamic factors and lake's morphometry

Due to the absence of wind and rivers, we will suppose that density-driven flows dominate water motion within sub-glacial Lake Vostok. Consideration must thus be given to (1) the effect of pressure on the temperature of maximum density; (2) the effect of pressure on the freezing temperature; (3) geothermal heating; (4) Coriolis effect; and (5) potential particle and gas fluxes from the overlying ice and their related mineralization and dissolution within the lake's water. In turn, the inclined ice ceiling may modify these factors.

The depression of the temperature of maximum density, T_{MD} (°C), with pressure p (dbar or 10^4 Pa) is given in the "linearized-form" by (see Fig. 1)

$$T_{\mathrm{MD}}(S,p) = T_{\mathrm{MD}}(S,0) - 0.00215p \quad (^{\circ}\mathrm{C}), \tag{1}$$

where S is the salinity (Chen and Millero, 1986). The depression of the freezing temperature, T_{FP}, with pressure is as follows (see Fig. 1):

$$T_{\mathrm{FP}}(S,p) = T_{\mathrm{FP}}(S,0) - 0.000753p \quad (^{\circ}\mathrm{C}) \tag{2}$$

(Fujino et al., 1974; UNESCO, 1978). Taking $T_{\mathrm{MD}}(0,0) \sim 3.984^{\circ}\mathrm{C}$ and $T_{\mathrm{FP}}(0,0) \sim 0^{\circ}\mathrm{C}$, we see that the two lines cross at a critical pressure $p_{\mathrm{Crit}} \sim 2840$ dbar $\{3.984/(0.00215 - 0.000753)\}$. This corresponds to an overlying ice-cover of about 3170 m thickness for an ice density of $\rho_{\mathrm{Ice}} \sim 913$ kg m^{-3} (Kapitsa et al., 1996; Fig. 1).

Two thermodynamic cases are now evident. First, for ice sheets thinner than the critical pressure p_{Crit} we have $T_{\mathrm{MD}} > T_{\mathrm{FP}}$. Adjacent to the ice ceiling, the temperature T of the lake water

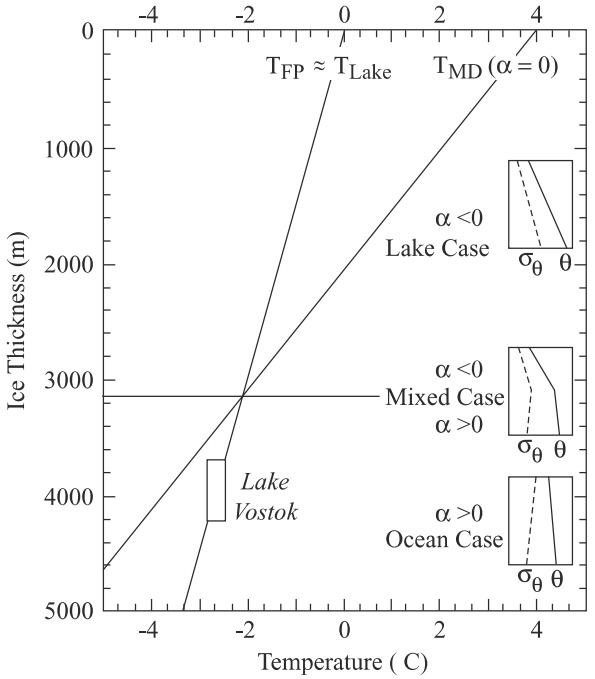

Fig. 1. Freezing temperature (T_{FP}) and temperature of maximum density (T_{MD}) as a function of ice thickness: Three types of lakes under ice can be expected in Antarctica, depending on whether the ice thickness is larger, lesser than or about equal to the critical depth (~3170 m depth for $\rho_{Ice} \sim 913$ kg m^{-3}), at which T_{FP} and T_{MD} are identical. In Lake Vostok (lake temperature ~−2.7°C) T_{FP} is warmer than T_{MD} (~−4°C) and the thermal expansivity α is positive (Ocean case); subsequently potential density σ_θ decreases as the potential temperature increases with depth (convectively unstable). In the Lake case σ_θ is stably stratified.

must be near T_{FP}. We therefore have $T_{MD} > T$, which implies that the thermal expansivity α (K^{-1}) $= -\rho^{-1}\partial\rho/\partial T < 0$. Hence, a *stable* density stratification occurs for geothermal heating from below (stability N^2 (s^{-2}) $= g\alpha\partial\theta/\partial z > 0$; $g = 9.81$ m s^{-2} is the gravitational acceleration; θ the potential temperature and z is the vertical coordinate, positive upwards). This is the classical situation of stratified freshwater lakes in winter with an inverse temperature gradient, so we therefore refer to this as the "Lake case" (Fig. 1). Second, for ice sheets thicker than p_{Crit}, as is the case in Lake Vostok, the sign changes: $T_{MD} < T_{FP}$, and therefore $T_{MD} < T$. Thus $\alpha > 0$ and an *unstable* water column results in geothermal heating from below ($N^2 < 0$). It is curious that the large pressure due to the floating ice plays the same role as salt in the ocean in suppressing T_{MD} below T_{FP}, and thus, in terms of convection, Lake Vostok behaves more like an ocean than a lake. We therefore refer to this ($\alpha > 0$) as the "Ocean case" (Fig. 1).

According to the ice thickness data on 77 Antarctic sub-glacial lakes listed by Siegert et al. (1996), 28 and 49 correspond to the Lake case and Ocean case, respectively. An interesting situation would arise if p_{Crit} were to lie within a lake water body yielding both types of stratification due to the changing sign of α within the water column. In fact, seven out of the above-mentioned 77 lakes do have an ice-cover thickness within a few meters of the critical pressure (Siegert et al., 1996) and will most probably yield this odd property. In the following, we concentrate on the

Ocean case type of Lake Vostok and review at the end the implications for the Lake case type of sub-glacial waters.

Combined data from airborne radio echo sounding, ERS-1 satellite altimetry (Siegert and Ridley, 1998) and seismic measurements (Kapitsa et al., 1996) provide rough estimates of the lake's morphometry and ice-cover (Table 1). A schematic section along the lake's main axis (with y positive towards the north) is shown in Fig. 2. The adjacent ice sheet flows onto the lake from the northwest and west at a speed of about 3 m a^{-1} (Kapitsa et al., 1996; Siegert and Ridley, 1998; Siegert et al., 2000). The ice sheet is significantly thicker over the lake's northern end (Siegert and Ridley, 1998; Fig. 9(a)): being 4.2 and 3.7 km thick over the northern and southern ends of the lake, respectively, the ice-cover thins towards south by ~460 m (Fig. 2). The top of the glacier has a north–south slope of ~40 m over the length of $L \sim 230$ km (~0.17 m km^{-1}). Thus an

Table 1
Lake Vostok's morphometry, ice cover and physical constants

Quantity	Symbol	Value
Lake		
Volume	V	1800 km^3
Area	A	14000 km^2
Length	L	230 km
North–south coordinate	y	0–230 km
Average width		60 km
Depth	$H(y)$	0–510 m
Average depth	H_{avg}	130 m
Maximum depth	H_{max}	510 m
Geothermal heat flux[a]	F_{geo}	0.050 W m^{-2}
Ice cover		
Ice thickness	$H_{Ice}(y)$	~3700–4200 m
Ice surface slope		0.17 m km^{-1}
Ice thickness difference (N–S)	ΔH_{Ice}	460 m
Ice ceiling[b] temperature at N-end	T_{Ice} $(y = L)$	−2.83°C
Ice ceiling[b] temperature at S-end	T_{Ice} $(y = 0)$	−2.53°C
Ice ceiling[b] temperature variation	ΔT_{Ice}	0.31 K
Constants		
Coriolis parameter (at 77°S)	f	-1.4×10^{-4} s^{-1}
Thermal expansivity of water[c]	α	18×10^{-6} K^{-1}
Heat capacity of water	$c_p\rho$	4.2×10^{6} J K^{-1} m^{-3}
Thermal diffusivity	D_T	1.35×10^{-7} m^2 s^{-1}
Gravitational acceleration	g	9.81 m s^{-2}
Adiabatic gradient[c]	Γ	1.1×10^{-5} K m^{-1}
Latent heat of melting	L_p	3.34×10^{5} J kg^{-1}
Kinematic viscosity	ν	2.0×10^{-6} m^2 s^{-1}
Ice density	ρ_{Ice}	913 kg m^{-3}
Water density[d]	ρ	1016 ± 1 kg m^{-3}

[a] See Salamatin et al. (1998).
[b] Temperature of the ice-ceiling in contact with the lake water, using Eq. (2).
[c] Average value.
[d] Assumption: salinity $S \sim 0$ (compressibility is included).

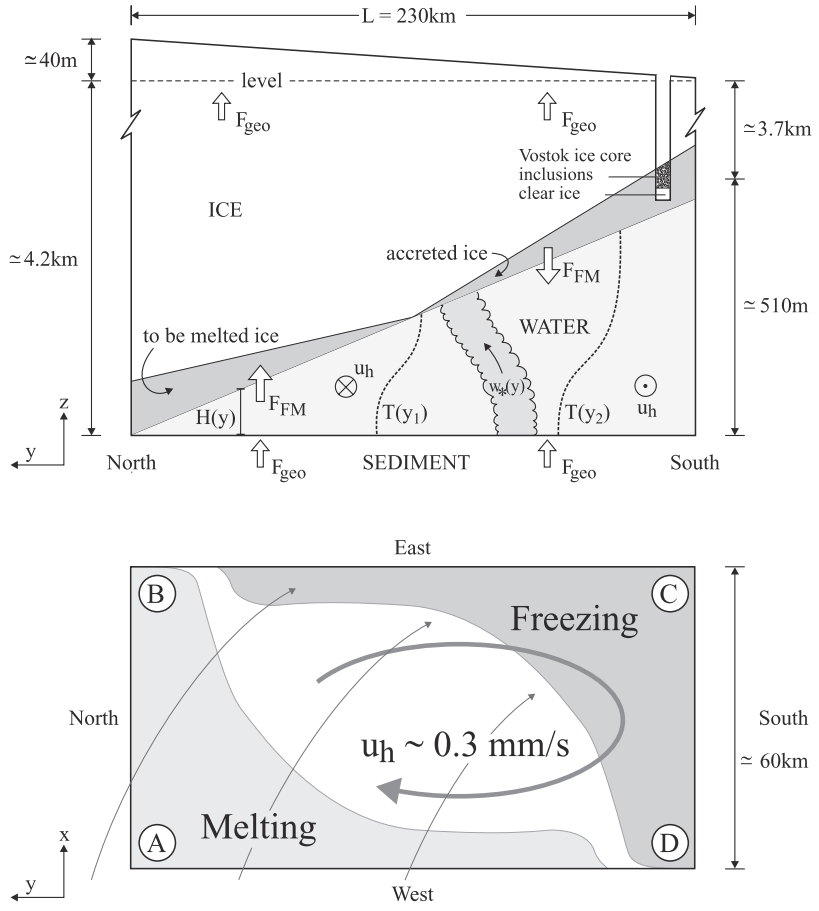

Fig. 2. Sketch of Lake Vostok's geometry, flow and ice-cover for parameters summarized in Table 2. The thin lines indicate the direction of the ice sheet flowing over the lake. Melting occurs at the thick-ice side (N) and at the west-margin; freezing at the thin-ice side (S) and east-margin. The horizontal convection is directed clockwise (heavy line). The plumes are tilted to the north (at the west side) and to the south (at the east, where subsequently isotherms are not exactly vertical). Isotherms $T(y_1) < T(y_2)$. The ice-core at the Vostok station (near C) is made of the climatic ice record (to 3539 m depth) and accreted ice at the lower end (below 3539 m). The upper section of the accreted ice contains particles (3539–3609 m depth).

independent check of the ice thickness variation can be made using the hydrostatic relation. In order to balance hydrostatic pressure the ice sheet must thicken from the southern to the northern end of the lake by $\{1 + \rho_{\mathrm{Ice}}/(\rho - \rho_{\mathrm{Ice}})\}40 \sim 400$ m (again $\rho_{\mathrm{Ice}} \sim 913$ kg m^{-3} is assumed), in good agreement with soundings. (The maximum depth of the lake water ($H_{\max} \sim 510$ m) calls for $(\rho/\rho_{\mathrm{Ice}})H_{\max} \sim 560$ m thicker ice sheet on the lake boundary to compensate the hydrostatic pressure.) In the following calculations, we choose the ice thickness difference as 460 m, which yields a temperature difference of $\Delta T_{\mathrm{Ice}} = 0.31$ K along the 230 km north–south section. We expect the ice ceiling temperature $T_{\mathrm{Ice}}(y)$ to be ΔT_{Ice} colder at the northern end than at the southern end.

Three observed features of the ice sheet are important for our analysis. First, the ERS-1 satellite altimetry reveals a remarkably flat surface terrain over the lake (Siegert and Ridley, 1998),

indicating that the irregularities of the ice thickness flowing onto the lake are smoothed out by some processes as the glacier glides over the lake (see below). Second, airborne 60 MHz ice penetrating radar reveals that the ice sheet, which flows from north–west and west towards east and south–east at a speed of about 3 m a^{-1}, looses ice at the lake's western and northern (thick-ice) parts, whereas the sheet gains ice at the southern and south-eastern (thin-ice) parts (Siegert et al., 2000; Fig. 2). Third, deep ice-core drilling indicates, consistent with freezing at the southern (down-flow) end of the lake, the presence of a 210 m thick layer of accreted lake water below the Vostok core site (Jouzel et al., 1999). This accreted lake water ice is made of two distinct layers. The upper 70 m contain visible inclusions consisting of inorganic particles, whereas the lower 140 m is extremely clear ice (Jouzel et al., 1999). The accreted ice contains neither dissolved solids nor air.

3. Hydrodynamics in lake Vostok

In the following section, we examine the scales of motion expected within Lake Vostok by discussing in the order of: (1) boundary conditions, (2) vertical thermal convection, (3) the heat internal balance, (4) horizontal convection, and (5) interactions between the lake and the ice ceiling.

3.1. *Boundary conditions*

Four boundary conditions are crucial for the internal dynamics of the Lake Vostok's water body:

- geothermal heat flux, F_{geo};
- freezing and melting and associated heat fluxes from/to the ice ceiling, F_{FM};
- absolute ice thickness, $H_{\mathrm{Ice}}(y)$;
- tilting of the ice ceiling (temperature difference along the tilted ice ceiling, ΔT_{Ice}).

In the following, we will show how these four parameters govern the lake's internal dynamics by evaluating the vertical and horizontal motions. Information and assumptions on boundary conditions, lake's morphometry and physical constants are listed in Table 1; whereas Table 2 summarizes the results of our a priori estimates.

The time scale for ice to pass over the width of the lake ($\sim$60 km) is about $\tau_{\mathrm{passage}} = 20\,000$ years (60 km at 3 m a^{-1}; Siegert et al., 2000). On this time scale one can expect the lake's volume and boundaries to change substantially. Since we do not know those boundary conditions (including the conductive heat loss through the ice) from observations, we make the following key assumptions. First, the heat flux through the lake is equal to the geothermal heat flux $F_{\mathrm{geo}} \sim 0.050$ W m^{-2} (Salamatin et al., 1998), and the lake is in steady state (i.e., the heat entering from below leaves the lake water at the ice ceiling; Fig. 2). This assumption implies that there is no net heating or cooling of the lake water. Second, at the down-flow (south and southeast) end of the lake the re-freezing of $\sim$150 m of ice takes place on a time scale of half of the ice passage over the lake (Siegert et al., 2000). This corresponds to a freezing rate of $E \sim 1.5$ cm a^{-1}, which is equivalent to a heat flux F_{FM} from the ceiling of $EL_{\mathrm{p}}\rho_{\mathrm{Ice}} \sim 0.15$ W m^{-2} (where $L_{\mathrm{p}} = 3.34 \times 10^5$ J kg^{-1} is the latent heat of freshwater ice); thus $F_{\mathrm{FM}} \sim 3F_{\mathrm{geo}}$. The second assumption allows the lake's

Table 2
Estimated physical properties of Lake Vostok

Quantity	Symbol	Value
Vertical convective turbulence		
Buoyancy flux	$J_b = (g\alpha/\rho c_p)F_{geo}$	1.5–2.6 × 10^{-12} W kg^{-1}
Convective velocity scale	$w_* = 2.4(J_b/f)^{1/2}$	0.3 mm s^{-1}
Eddy viscosity	$K_{con} = w_* H/2$	200 cm^2 s^{-1}
Vertical temperature gradient	$\partial\theta/\partial z$	6×10^{-7} K m^{-1}
Adiabatic temperature gradient	Γ	1.1×10^{-5} K m^{-1}
Horizontal convection		
Thermal diffusive sub-layer ($y > L/2$)	δ_M	6 cm
Thermal diffusive sub-layer ($y < L/2$)	δ_F	~0.7 m
Convective velocity scale	u_h	0.34 mm s^{-1}
Heat flux melting ($y > L/2$)	F_{FM}	~0.25 W m^{-2}
Heat flux freezing ($y < L/2$)	F_{FM}	~−0.15 W m^{-2}
Horizontal temperature gradient	$\partial T/\partial y$	5×10^{-7} K m^{-1}
Time scales		
Ice passage	$\tau_{passage}$	20 000 a
Lake water recycling by melting/freezing[a]	$H_{avg}/(0.5E)$	17 000 a
Vertical convection	$\tau_{con} = H_{avg}/w_*$	5 d
Horizontal convection	$2L/u_h$	45 a
Temperature adjusting	$\tau_{adj} = \delta_M H_{avg}/D_T$	2 a

[a] Melting rate $E = 1.5$ cm a^{-1} (150 m during half a passage of 20 000 a). The factor of 0.5 arises since water is added (by melting) over the northern half of the lake, whereas water is withdrawn (by freezing) in the southern half of the lake.

volume to vary on geological time scales, since the Lake Vostok water residence time due to the melting/freezing cycle is only $H_{avg}/(0.5E) \sim 17\,000$ years (average lake water depth $H_{avg} = 130$ m; Table 1), which is roughly equal to the ice passage. Thus, whereas the phenomenon of the subglacial lake may be old (millions of years), the lake's volume most probably is variable. The "age" of the water is given by the age of the glacier base (400 ka; Petit et al., 1999), while the actual water residence in the lake is relatively short (thousands of years).

3.2. *Vertical thermal convective turbulence*

The scaling of convection is determined by the height of the convecting layer, the buoyancy flux J_b and the Coriolis parameter (Fernando et al., 1991; Marshall and Schott, 1999). The convecting-layer height will vary according to the thickness $H(y)$ of the lake water body (Table 1). In steady state, the lake's average *internal* heat flux is identical to the geothermal flux F_{geo}, and the buoyancy flux is given by

$$J_b = \frac{g\alpha}{\rho c_p} F_{geo} = 1.5\text{–}2.6 \times 10^{-12} \quad (\mathrm{W\ kg^{-1}}), \tag{3}$$

where $c_p\rho \sim 4.2 \times 10^6$ J K^{-1} m^{-3} is the heat capacity of freshwater (pressure-dependence neglected). J_b is proportional to the pressure-dependent thermal expansivity $\alpha(p) =$

$15.6 \times 10^{-6}(T - T_{MD}(p))$ (K^{-1}), which varies from 13–22 $\times 10^{-6}$ K^{-1} within the lake. Here an average of $\alpha \sim 18 \times 10^{-6}$ K^{-1} is used. The randomly rising and sinking convective plumes have vertical velocities of (Fernando et al., 1991)

$$w_* = 2.4(J_b/f)^{1/2} \sim 0.3 \quad (\text{mm s}^{-1}). \tag{4}$$

Although this velocity may appear very small, the effect of w_* is to allow very efficient vertical mixing within the lake water body. The time scale for a thermal plume to cover H_{avg} is only $\tau_{con} = H_{avg}/w_* \sim 5$ days, which is instantaneous compared to the age of the lake or the passage of the ice sheet (Table 2). Furthermore, due to the high vertical turbulent diffusivity of $K_{con} = w_* H_{avg}/2 \sim 200$ cm^2 s^{-1}, the vertical gradients of potential temperature can be expected to be extremely small. The potential temperature (θ) will increase with depth at a rate of $\partial\theta/\partial z = F_{geo}/(c_p \rho K_{con}) \sim 6 \times 10^{-7}$ K m^{-1}; thus vertical potential temperature differences over the lake's depth of $\Delta\theta = \partial\theta/\partial z H_{avg} \sim 0.08$ mK are to be expected. The observable in situ temperature gradient would consequently be determined by the adiabatic gradient $\Gamma = g\alpha(T + 273.15)/c_p = 1.1 \times 10^{-5}$ K m^{-1} (corresponding to $\Delta T = \Gamma H_{avg} \sim 1.5$ mK). Therefore, a temperature sonde would observe an increase of the in situ temperature from the ice ceiling towards the bottom of the lake up to ~6 mK (ΓH_{max}), values which are extremely small but still detectable with commercial CTDs. As discussed below, the potential temperature gradients $\partial\theta/\partial z$ will show an asymmetry in the west–east direction due to the Coriolis deflection.

Other lake properties can potentially influence the net buoyancy flux, and require discussion. For example, in the northern part of the lake, particles are continuously added to lake water at the top of the water column, due to melting (Fig. 2) and the subsequent release of entrapped atmospheric particles and glacial till and flour (see Petit et al., 1999). By assuming that the ~500 m thick sediment layer has been deposited over a time span of 10 million years, we calculate a particle "rain" of $\sim 2.2 \times 10^{-9}$ kg m^{-2} s^{-1}, which corresponds to a buoyancy flux of $\sim 1.3 \times 10^{-11}$ W kg^{-1}, about 10 times that due to geothermal heating. Most of the sediment mass can be expected to be made of glacial rubble and particles large enough to sink much faster than 0.3 mm s^{-1} (and therefore not contributing to convective turbulence). However, the μm-particles and sub-μm colloids do add to convective mixing under the melting ice section. Further, as a result of convective turbulence, particles sinking slower than 0.3 mm s^{-1} (corresponding to a Stokes particle size of ~20 μm) will remain long in the water column. Vostok may thus be expected to be turbid, visually much like a glacially fed intermontane lake.

If the lake's volume has been present for a sufficiently long time, salts and dissolved gases may have built up the lake water. It is safe to assume that the salinity is low, since even if the lake has resided for millions of years, the accumulated salts would still be only a few per mill. Due to the intermittent behavior of climate, the lake's cavity has likely disappeared on occasion over the time span of 20 million years. In any case, melting will add salts and dissolved gases (90 ml kg^{-1} ice) at the northern part (thick-ice), and both affect the buoyancy flux. Both gas and salt concentrations are lower in the newly melted water than the ambient lake water; hence the gases generate positive buoyancy flux (producing convection and turbulence), and the salts will produce negative buoyancy flux (suppressing convection and turbulence). Both contributions are less important than the thermally induced convective turbulence.

3.3. *Heat balance*

The steady-state assumption of no net melting/freezing implies that at present the heat entering the lake water from below (right-hand side of Eq. (5)) leaves the water through the ice ceiling (left-hand side of Eq. (5))

$$\int_{y=0}^{y=L} c_p \rho D_T \frac{T(y) - T_{Ice}(y)}{\delta(y)} \, dy = \int_{y=0}^{y=L} F_{FM}(y) \, dy = F_{geo} L \quad (W \ m^{-1}), \tag{5}$$

where D_T (1.35×10^{-7} m^2 s^{-1}) is the molecular thermal diffusivity (pressure-dependence neglected) and $\delta(y)$ is the thickness of the thermal diffusive sub-layer below the ice ceiling. We know the ice ceiling temperature $T_{Ice}(y)$ to be close to freezing temperature $T_{FP}(p(y))$ of the local pressure p, i.e., $T_{Ice}(y) = T_{FP}(p(y))$. As noted above, vertical mixing is fast and therefore $T(y,z)$ varies little along z and is almost entirely a function of the north–south coordinate y, i.e., $T(y) \sim T(y,z)$. Observations by radar echo sounding reveal that ice melts at the up-flow end (thick-ice in Fig. 2; $F_{FM} > 0$ is directed out of the water), and water freezes at the down-flow end (thin-ice in Fig. 2; $F_{FM} < 0$ is directed into the water).

The temperature $T(y)$ is further dependent on the heat balance in the interior of the water body. Again, for steady state, the horizontally transported heat through a vertical x–z cross-section at y (left-hand side in Eq. (6)) has to balance the fluxes through the lake bottom and ice ceiling of the water volume on either side of the cross-section (right-hand side in Eq. (6))

$$\int_{z=0}^{z=H(y)} \int_{x=0}^{x=\mathrm{Width}} c_p \rho u(y,x) T(y,x) \, dx \, dz = y F_{geo} - \int_{y'=0}^{y'=y} F_{FM}(y') \, dy' \quad (W \ m^{-1}). \tag{6}$$

In Eq. (6), the horizontal heat flux due to turbulent diffusion ($c_p \rho K_{con} \partial T(y)/\partial y$) has been neglected, as it is much smaller than the advective heat flux. If there were no horizontal transport (i.e., vertical convective turbulence only), the temperature at position y in the lake would almost be at $T_{Ice}(y)$ (in fact slightly warmer) and consequently the horizontal temperature gradient would be $\partial T(y)/\partial y \sim \partial T_{Ice}(y)/\partial y \sim 1.3 \times 10^{-6}$ K m^{-1} (or $\Delta T_{Ice} = 0.31$ K over $L = 230$ km). Any horizontal heat exchange, however, reduces the horizontal temperature gradient and thereby increases the water temperature at the cooler (thick-ice; north) side, whereas vice versa the temperature at the warmer (thin-ice, south) side decreases. As a result, the temperature at the thick-ice side is $T(y) > T_{Ice}(y)$ (consistent with local melting) and vice versa at the thin-ice side $T(y) < T_{Ice}(y)$ (consistent with local freezing). Although, horizontal mixing is not the primary reason for melting and freezing, it is not counteracting and rather supporting the melting/freezing segregation along y.

3.4. *Horizontal convection*

Horizontal convection is generated due to the pressure gradient $\partial p/\partial y = gH(y)\rho\alpha\partial T(y)/\partial y$, effected by the horizontal temperature gradient. Since both, $\partial T(y)/\partial y$, as well as α are very small, the density difference $\Delta\rho/\rho = \alpha L \partial T(y)/\partial y$ along the lake is very small compared to other natural water bodies (Table 2). For steady state this baroclinic pressure gradient $\partial p/\partial y$ is balanced by Coriolis force and internal friction

$$\frac{\partial v}{\partial y} = -fu - \frac{\partial p}{\rho \partial y} + \frac{\partial}{\rho \partial z}\left(A_{\text{turb}} \frac{\partial u}{\partial z}\right) = 0 \quad (\text{s}^{-1}), \tag{7}$$

where f is the Coriolis parameter (-1.4×10^{-4} s^{-1}; Table 1). For scaling purposes, we set the turbulent viscosity $A_{\text{turb}} \sim K_{\text{con}}$. This approximation is justified, because convective turbulence is active (not suppressed by buoyancy) and consequently the turbulent Prandtl number is close to unity. Since in Eq. (7) friction is much smaller than the Coriolis force ($A_{\text{turb}}/\{H_{\text{avg}}^2 f\} \ll 1$), we neglect internal friction. Eqs. (6) and (7) then allow calculating the solution for a given set of boundary conditions and geometry. Balancing the heat flux at $y = L/2$ by using Eq. (6)

$$4F_{\text{geo}} = c_{\text{p}} \rho u_{\text{h}} \partial T/\partial y (H_{\max}/2) \quad (\text{W m}^{-2}) \tag{8a}$$

and the momentum, by applying Eq. (7)

$$u_{\text{h}} = (gH_{\max}/f)\alpha \partial T/\partial y \quad (\text{m s}^{-1}) \tag{8b}$$

leads to estimates for the horizontal current speed of $u_{\text{h}} = \{8F_{\text{geo}} g\alpha/(c_{\text{p}}\rho f)\}^{1/2} = 0.34$ mm s^{-1} and for $\partial T/\partial y = \{8F_{\text{geo}} f/(g\alpha c_{\text{p}} \rho H_{\max}^2)\}^{1/2} = 5 \times 10^{-7}$ K m^{-1} (0.12 K per 230 km). The horizontal convection corresponds to a volume flux of 1300 m^3 s^{-1}, which is equivalent to a convection time scale of 45 years (lake volume per volume flux). This implies a fast reaction of the horizontal convection to changing climatic conditions at the ice ceiling. Comparably, the melting/freezing water flux is only 3 m^3 s^{-1}.

Due to details not considered (including geometry), the scaling in Eqs. (8a) and (8b) may be off by a factor of O(1). For confirmation we note that another means for setting an upper limit on the horizontal velocity scale follows from energy conservation, which requires energy dissipation $K_{\text{con}}(\partial u/\partial z)^2$ to be smaller than the driving energy source in the form of the buoyancy flux J_{b}. Assuming a mixing ratio (the ratio between the rate of change of potential energy to the turbulent production of kinetic energy) for convection of

$$\gamma_{\text{mix}} = K_{\text{con}}(\partial u/\partial z)^2/J_{\text{b}} \sim 0.2 \quad (\text{dimensionless}) \tag{9}$$

(cf. Ivey and Imberger, 1991) yields an upper limit for the velocity scale of 0.6 mm s^{-1}, consistent with that found using Eqs. (8a) and (8b).

The effect of horizontal convection is to reduce the horizontal temperature gradient $\partial T(y)/\partial y$ below the gradient $\partial T_{\text{Ice}}(y)/\partial y$, imposed by the ice ceiling. The steady state of the horizontal convection is such that it balances simultaneously the baroclinic pressure gradient and satisfies the internal heat balance. The latter determines the clockwise direction of the circulation, for which the heat transport will be most efficient, given the melting/freezing pattern in Fig. 2. Both, the melting/freezing rates as well as the tilting of the ceiling determine the scale of the internal convection.

3.5. *Interaction between lake water and ice ceiling*

On the thick-ice side the lake water $T(y)$ is only slightly warmer than the ice, whereas on the thin-ice side the lake water is substantially cooler than the ice (Table 2). The difference between $T(y)$ and $T_{\text{Ice}}(y)$ is not symmetrical along y for the following arguments. For $y > L/2$ (north) the vertical heat flux ($5F_{\text{geo}}$) forces convective turbulence to rise to the ice ceiling. Here the thickness of

the thermal diffusive sub-layer $\delta(y)$ depends on the level of the convective turbulence and on currents along the ice ceiling. For the first process, $\delta(y)$ is given by the smallest scales of turbulent temperature variations, the so-called Batchelor scale, $\delta_M = 2\pi(\nu D_T^2/J_b)^{1/4}$ ($\sim$0.06 m) where ν is the kinematic viscosity (index "M" indicates the zone of "melting"). Since the horizontal velocities u_h are very small the corresponding thermal diffusive sub-layer ($\sim 10\ (\nu/u_*)(D_T/\nu)^{1/2}$, where u_* is the friction velocity; Hinze, 1975) is larger than the Batchelor scale. Subsequently, convective turbulence defines the limiting eddy size for molecular heat exchange at the ice ceiling. For $y > L/2$ a thermal sub-layer of thickness $\delta_M \sim 0.06$ m will build up along the ceiling, within which the temperature drops from $T(y)$ in the lake water to $T_{Ice}(y)$ at the ice by $5F_{geo}\delta_M/(D_T c_p \rho) \sim 0.026$ K.

For $y < L/2$ (freezing in the down-flow zone of the lake) the heat flux at the ceiling is towards the water, which causes stable stratification close to the ice ceiling. Evidence for this comes from the thickness of the molecular interface at $y = 0$, where $\delta_F = D_T c_p \rho\{T_{Ice}(0) - T(L) - L\partial T/\partial y\}/(3F_{geo}) \sim 0.7$ m (index "F" indicates the zone of "freezing"). There, at the lake's maximum water depth, we can expect a small pool of slightly warmer ($T_{Ice}(0) - T(L) - L\partial T/\partial y \sim 0.17$ K) and stably stratified water below the ice ceiling.

It is noteworthy to mention that circulation in the lake is driven by the prescribed heat fluxes and the tilting of the ice ceiling. The effect of the resulting circulation is that it supports the reshuffling of ice from the thick-ice layer towards the thin-ice layer. As long as there is a temperature gradient in the water the subsequent baroclinic pressure gradient leads to convection, which transports heat from the thin-ice side to the thick-ice side and subsequently helps to level the tilted ice sheet. When the "ice pump", however, would come to rest, depends primarily on the lateral distribution of the ice temperature at the base of the ice sheet and cannot be predicted. Melting rates, proposed by Lewis and Perkin (1986) and McPhee (1983) allow us to estimate the amount of ice expected to be reshuffled. For the temperature differences $T(y) - T_{Ice}(y)$ and the horizontal current $u_h \sim 0.34$ mm s^{-1} their relations predict between 50 and 200 m of ice (depending on the detailed geometry of the flow) relocated for the time scale of the ice passage. This comparison, although most probably overextending the range of applicability, confirms the approximate volumes of ice melted and reallocated by the internal ice pump.

Changes in the thickness of the inflowing ice or variations of the ice temperatures cause the water temperature to deviate from steady-state equilibrium. The time scale of adjustment $\tau_{adj}(y) = \delta_M H(y)/D_T$ is proportional to the depth $H(y)$ of the water column and the thickness of the molecular ice–water boundary and reaches a maximum of 80 years at the deepest location of the lake, but is on average only 2 years. Again, this implies that water column adjustment is fast compared to the passage of the ice over the lake (Table 2). ERS-1 satellite altimetry reveals that the ice surface is extraordinarily and almost perfectly flat, which coincides exactly with the lake boundary known from radar and seismic observations (Siegert and Ridley, 1998). It seems therefore quite obvious to hypothesize that such smoothness is related to the presence of the sub-glacial water. Let us assume an ice block of 1 m height irregularity moves onto and across the lake. Hydrostatic adjustment calls for 91% of this irregularity to "dive" at the ice ceiling, leading to a 0.91 m thick irregularity at the ice ceiling. Geothermal heating would eliminate such an irregularity within 175 years, about 100 times faster than the passage of the ice sheet over the lake. This implies that during the time ice crosses the lake, melting and freezing are able to smoothen out irregularities of tens of meters, producing the stunningly flat ice that extends over the lake.

4. Discussion and conclusions

A summary of what we can expect in terms of physical processes while exploring Lake Vostok is given in Table 2. The lake water will definitely *not* be at rest and transport and mixing will far exceed molecular levels. Two types of internal motions can be expected: (a) convective vertical plumes with velocity scales of $\sim$0.3 mm s^{-1}; and (b) horizontal convection of the same magnitude driven by baroclinic pressure gradients consistent with momentum and energy conservation, whereas the vertical convective turbulence is mainly dependent of the geothermal heat flux, the key parameters for the horizontal circulation are the prescribed (based on observation) heat fluxes for melting and freezing, and the tilting of the ice ceiling. The phenomenon that tilting can cause horizontal convection, is not restricted to this application, as shown by Gill and Turner (1969) for a double-diffusively stratified water body of varying depth.

Vertical mixing can be expected to be very fast, efficiently eliminating density differences in the vertical on a time scale of days. Changes in the behavior of the circulation will occur over time scales of a few decades, defined by the time scales of temperature adjustment (<1 decade), circulation time scale (several decades) and the time scale of removal of ice roughness elements (century). Due to the continuous addition of atmospheric and glacial particles, the water column will become very turbid, since convective turbulence will keep $\sim$20 μm particles and smaller ones in suspension.

The presented model explains well the strange third feature of the ice-cover mentioned in Section 2. Jouzel et al. (1999, see Fig. 3) found inorganic particles in the upper section of the accreted ice. This is exactly what our model predicts. As the ice sheet moves over the lake, freezing (accretion) begins at about the central region of the lake. There, vertical convective turbulence is reaching all the way to the ice ceiling, attaching inorganic particles from the turbid water column. As the ice sheet reaches the southern part, an m-thick molecular boundary layer builds up (due to freezing-induced heating from above) and the geothermal convection cannot hit the ice ceiling anymore. The ice accretion becomes a purely molecular process and leads to perfectly clear ice with very low partition ratios (no salt, no gas, and no particles), as observed by Jouzel et al. (1999). Also microorganisms are much more likely to be found in the upper section of the ice, which was accreted over turbulent lake water.

In the horizontal, however, there will remain a density difference, which is $\sim$1/3 of the one imposed by the pressure-dependent freezing temperature $T_{\mathrm{FP}}(p)$ along the tilted ice ceiling. The effect of the resulting circulation will lead to temperature and density isolines with a large inclination angle; that is, plumes will rise and sink not vertically but rather at an angle of order $\sim$45°. As a result tilted thermals will warm up and cool off by $\Delta\theta \sim \pm 0.05$ mK as they rise on the east and west side of the ice sheet, respectively (Fig. 2). A high-resolution temperature profiler will therefore "see" the combined effect of the convectively unstable temperature profile ($\Delta\theta \sim 0.05$ K) and the tilted plumes ($\Delta\theta \sim \pm 0.05$ mK) while lowered over the depth of the lake. Whereas on the west side of the sheet θ will be almost constant, θ will increase by about 0.1 mK towards the bottom on the east side. The observable in situ temperature will however, increase towards the bottom due to adiabatic compression over the lake depth by up to 6 mK at the deepest position, well resolvable for a commercial CTD.

Melting at the "thick-ice" side (north) and freezing at the "thin-ice" side (south) of up to 150 m drives the internal circulation and internal heat flux as the ice sheet passes over the lake. These

internal heat fluxes remove topographic irregularities on time scales much shorter than the ice passage time. This corroborates well with the observation that the ice surface is extraordinarily flat. The general shape of the ice sheet however (460 m thicker at the northern end) reflects the N–S structure of the thickness of the inflowing ice and is for sure not related to the internal ice pump, which tends to level the ice ceiling.

Under steady state, other water constituents would likely be well mixed, lacking vertical gradients in particles, salinity, and dissolved nutrients (except a very small volume below the ceiling where the lake is deepest). We are uncertain, however, of expected gradients of pH and concentration of gases, which may be affected by pressure and the related formation of clathrate air-hydrate crystals (Uchida et al., 1994; Salamatin et al., 1998). If the lake were not in steady state (quite possible) and e.g., still melting, there would be probably no accumulation of salt or other chemicals (it seems that the water is of fresh origin, no salt-water intrusions). If more ice were to melt within the lake, some "spilling over" and re-freezing could occur below the southern end. Or during cold episodes, the lake's cavity could be removed by the glacier altogether. This might transport microorganisms from the lake into the down-flowing ice, and one cannot assume that Lake Vostok water is fully sealed from the surrounding land and atmosphere.

Our present analysis has dealt only with the Vostok cavity. We note, however, that there are at least 77 other sub-glacial lakes in Antarctica (Siegert et al., 1996). Beside the Ocean case discussed above, there remain two other types of mixing regimes of sub-glacial lakes in Antarctica. For ice-cover less than the critical thickness of 3170 m, we face the Lake case ($\alpha < 0$), which remains stably stratified under geothermal heating and vertical convective turbulence is absent. The horizontal convection will occur in thin intrusion-type layers, transporting heat to the adjacent ceiling. As the "water at the thick-ice" end will be warmed up by the geothermal heating at a much faster rate than at the "shallow-ice" end, and since the pressure-dependent freezing temperature is lowest at the thick-ice end, melting will be most intense there. The difference with the Ocean case is that the water coming in contact with the melting ice will rise along the ceiling as it gets progressively cooler and thereby lighter. As the water body is stratified in the interior (much more than in the Ocean case), this boundary-plume will generate intrusions, which drive a horizontal heat flux. As in the Ocean case, this process will level out the ceiling, probably at a faster rate. Ceilings of Lake case sub-glacial lakes will therefore potentially be more level (however, depending on the temperature distribution of the inflowing ice).

If the ice-cover is slightly less than the critical thickness, the Ocean case and Lake case are both present within the lake water. In this "bimodal case" we expect unstable stratification in the lower part of the lake and stable stratification in the upper.

Many examples are found elsewhere in nature where extreme pressures (the geophysical squeeze-play) may affect water stratification and motion; e.g., in the oceans off Antarctic ice shelves (Carmack and Foster, 1975) and in deep lakes such as Baikal (Weiss et al., 1991). We also note that this analysis may be applicable to extraterrestrial bodies having liquid water covered by ice, such as Jupiter's moons Europa and Callisto. Prior to in situ measurements of circulation in Lake Vostok, possible scales of motion should be further explored, and we invite dialog. We also advocate field experiments to see if flow can be detected in similar but less extreme high pressure and low temperature situations (e.g., beneath the Ward Hunt Ice shelf off Ellesmere Island, Canada (see Jefferies, 1992).

Acknowledgements

We are indebted to Chris Garret, Trevor McDougall and an anonymous reviewer for very helpful comments on an earlier version of the manuscript and to G. Wagner and G. Zumofen for the assistance on understanding the ice above. The first author would like to thank the Institute of Ocean Sciences and in particular Eddy Carmack and David Farmer for their hospitality while on sabbatical in Sidney (BC, Canada). The second author would like to thank Frank Carsey for introducing him to mysterious Lake Vostok.

References

Carmack, E.C., Foster, T.D., 1975. Circulation and distribution of oceanographic properties near the Filchner ice shelf. Deep-Sea Res. 22, 77–90.

Chen, C.T., Millero, F.J., 1986. Precise thermodynamic properties for natural waters covering only the limnological range. Limnol. Oceanogr. 31, 657–662.

Fernando, H.J.S., Chen, R., Boyer, D.L., 1991. Effects of rotation on convection turbulence. J. Fluid. Mech. 228, 513–547.

Fujino, K., Lewis, E.L., Perkin, R.G., 1974. The freezing point of sea water at pressure up to 100 bars. J. Geophys. Res. 79, 1792–1797.

Gill, A.E., Turner, J.S., 1969. Some new ideas about the formation of Antarctic bottom water. Nature 224, 1287–1288.

Hinze, J.O., 1975. Turbulence. McGraw-Hill, New York, 618 pp.

Ivey, G.N., Imberger, J., 1991. On the nature of turbulence in a stratified fluid. Part I: The energetics of mixing. J. Phys. Oceanogr. 21, 650–659.

Jefferies, M.O., 1992. Arctic ice shelves and ice islands: Origin, growth and disintegration, physical characteristics, structural-stratigraphic variability, and dynamics. Rev. Geophys. 30, 245–267.

Jouzel, J., Petit, J.R., Souchez, R., Barkov, N.I., Lipenkov, V.Y., Raynaud, D., Stievenard, M., Vassiliev, N.I., Vimeuz, F., 1999. More than 200 m of lake ice above sub-glacial Lake Vostok, Antarctica. Science 286, 2138–2140.

Karl, D.M., Bird, D.F., Björkman, K., Houlihan, T., Shackelford, R., Tupas, L., 1999. Microorganisms in the accreted ice of Lake Vostok, Antarctica. Science 286, 2144–2147.

Kapitsa, A.P., Ridley, J.K., Robin, G.de Q., Siegert, M.J., Zotikov, I.A., 1996. A large deep freshwater lake beneath the ice of central East Antarctica. Nature 381, 684–686.

Lewis, E.L., Perkin, R.G., 1986. Ice pumps and their rates. J. Geophys. Res. 91, 11756–11762.

Marshall, J., Schott, F., 1999. Open-ocean convection: Observations, theory, and models. Rev. Geophys. 37, 1–64.

McPhee, M.G., 1983. Turbulent heat and momentum transfer in the oceanic boundary layer under melting pack ice. J. Geophys. Res. 88, 2827–2835.

NSF, 1999. Lake Vostok: A Curiosity or a focus for interdisciplinary study? Lake Vostok Workshop, Final Report, 7/8 November, NSF Washington DC, 15 June. On web at: http://www.ldeo.columbia.edu/vostok/.

Petit, J.R., Jouzel, J., Raynaud, D., Barkov, N.I., Barnola, J.-M., Basile, I., Benders, M., Chappellaz, J., Davis, M., Delaygue, G., Delmotte, M., Kotlyakov, M.E., Legrand, M., Lipenkov, V.Y., Lorius, C., Pepin, L., Ritz, C., Saltzman, E., Stievenard, M., 1999. Climate and atmospheric history of the past 420,000 years from the Vostok ice core, Antarctica. Nature 399, 429–436.

Priscu, J.C., Adams, E.E., Lyons, W.B., Voytek, M.A., Mogk, D.W., Brown, R.L., McKay, C.P., Takacs, C.D., Welch, K.A., Wolff, C.F., Kirshtein, J.D., Avci, R., 1999. Geomicrobiology of sub-glacial ice above Lake Vostok, Antarctica. Science 286, 2141–2144.

Salamatin, A., Vostretsov, R., Petit, J., Lipenkov, V., Barkov, N., 1998. Geophysical and paleo-climatic implications of the stacked temperature profile from the deep borehole at Vostok Station, Antarctica. Materially Glyatsiologicheskikh Isslefovanii 85, 233–240.

Siegert, M.J., Dowdeswell, J.A., Gorman, M.R., McIntyre, N.F., 1996. An inventory of Antarctic sub-glacial lakes. Antarctic Sci. 8, 281–286.

Siegert, M.J., Ridley, J.K., 1998. An analysis of the surface and sub-surface topography of the Vostok Station sub-glacial lake, central East Antarctica. J. Geophys. Res. 103, 10195–10207.

Siegert, M.J., Kwok, R., Mayer, C., Hubbard, B., 2000. Water exchange between the sub-glacial Lake Vostok and the overlying ice sheet. Nature 403, 643–646.

Uchida, T., Duval, P., Lipenkov, V., Hondoh, T., Mae, S., Shoji, H., 1994. Brittle zone and air-hydrate formation in polar ice sheets. Mem. Matl. Inst. Polar Res. 49, 298–305.

UNESCO, 1978. Eighth report on the joint panel on oceanographic tables and standards, Woods Hole, 23–25 May 1977. UNESCO Technical Papers in Marine Science 28.

Weiss, R.F., Carmack, E.C., Koropalov, V., 1991. Deep-water renewal and biological production in Lake Baikal. Nature 349, 665–669.